Initial gut microbial composition as a key factor driving host response to antibiotic treatment, as exemplified by the presence or absence of commensal *Escherichia coli*

Tingting Ju[a], Yasmeen Shoblak[a], Yanhua Gao[a*], Kaiyuan Yang[a], Janelle Fouhse[a], B. Brett Finlay[b], Yee Wing So[a], Paul Stothard[a], and Benjamin P. Willing[a#]

Department of Agricultural, Food and Nutritional Science, University of Alberta, 4-10 Agriculture/Forestry Centre, Edmonton, AB, Canada[a]

Michael Smith Laboratories, The University of British Columbia, Vancouver, British Columbia, Canada, Department of Microbiology and Immunology, The University of British Columbia, Vancouver, British Columbia, Canada[b]

Running title: Initial gut microbes affect response to antibiotics

*Present address: Yanhua Gao, College of Life Science and Technology, Southwest University for Nationalities, Chengdu, 610041, China

#Corresponding author footnote

3-10D Ag/For Centre

Edmonton, AB T6E 2P5, Canada

Phone: +1 7804928908

Email: willing@ualberta.ca

Abstract

Antibiotics are important for treating bacterial infection, however, efficacy and side effects of antibiotics vary in medicine and experimental models. A few studies correlated microbiota composition variations with health outcomes in response to antibiotics, however, no study has demonstrated causality. We had noted variation in colonic expression of c-type lectins, regenerating islet-derived protein 3 (*Reg3β*) and *Reg3γ*, after metronidazole treatment in a mouse model. To investigate causality of specific variations in pre-existing microbiome on host response to antibiotics, mice harbouring a normal microbiota were allocated to 4 treatments in a 2x2 factorial arrangement with or without commensal *Escherichia coli*; and with or without metronidazole in drinking water. *E. coli* colonized readily without causing a notable shift in microbiota or host response. Metronidazole administration reduced microbiota biodiversity, indicated by decreased Chao1 and Shannon index, and altered microbiota composition. However, presence of *E. coli* strongly affected metronidazole-induced microbiota shifts. Remarkably, this single commensal bacterium in the context of a complex population led to variations in host response to metronidazole treatment including increased expression of antimicrobial peptides *Reg3β* and *Reg3γ*, and intestinal inflammation indicated by tumor necrosis factor-alpha. Similar results were obtained from 2 week antibiotic exposure and with additional *E. coli* isolates. This proof of concept study indicates that even minor variations in initial commensal microbiota can drive shifts in microbial composition and host response after antibiotic administration. As well as providing an explanation for variability in animal models using antibiotics, the findings encourage the development of personalized medication in antibiotic therapies.

Key words. *Escherichia coli*, metronidazole, gut microbiota, regenerating islet-derived protein 3β (*Reg3β*), regenerating islet-derived protein 3γ (*Reg3γ*)

The importance of the study

This work provides an understanding of variability in studies where antibiotics are used to alter the gut microbiota to generate a host response. Furthermore, although only providing evidence for the one antibiotic, the study demonstrated that initial gut microbial composition is a key factor driving host response to antibiotic administration, creating a compelling argument to consider personalized medication based on individual variation in gut microbiota.

INTRODUCTION

Antibiotics have been extensively used in therapy of human and animal infections. The rational mechanisms of antibiotic therapies include decreasing bacterial density, eliminating targeted detrimental bacteria, inhibiting secondary bacterial proliferation, and reducing bacterial translocation, however, at the expense of strong alteration in the commensal microbiota (1). It is well-known that antibiotics have strong effects on the gut microbiota, resulting in imbalances of the microbial ecosystem and concomitantly affecting host physiology, particularly involving innate defense mechanisms (2–4). Antibiotic treatment that might help one individual can cause adverse outcomes in another (5). For instance, in inflammatory bowel disease (IBD) trials, the antibiotic therapies using metronidazole and ciprofloxacin resulted in contradictory outcomes (6–8). Moreover, the compositional changes of gut commensal microbiota in response to antibiotic therapies are variable between individuals. A large cohort study showed variation in the diversity and richness of antibiotic resistance genes in the human gut microbiota, which indicated the differences in altered microbiota by antibiotic usage (9). Administration of 500 mg ciprofloxacin twice a day for 5 days affected about 30% of bacterial taxa in the gut, however, with interindividual variation in the magnitude of the effects (10, 11). The mechanisms by which antibiotic administration leads to inconsistent host outcome are not entirely clear.

Several studies have illustrated the importance of monitoring the initial composition of gut microbiota prior to antibiotic administration. A recent human study, which recruited 18 healthy volunteers to take a therapeutic dosage of the antibiotic cefprozil for a week, showed that a subset of participants had a dramatic increase of a specific group of bacteria in response to antibiotic treatment. The subset were participants who initially categorized as a *Bacteroides* enterotype with lower microbial diversity (12). While the study pointed out the necessity of monitoring initial microbial composition, it did not provide direct evidence of variations in host response resulting from the initial differences in microbiota. The understanding of the host response underlying functional changes in the microbiota responding to antibiotic treatments remains limited, primarily because most studies to date have focused on compositional changes in microbiota and fail to provide information on corresponding changes in host response.

Our previous independent studies showed contradictory results for host gene expression of *MUC2*, regenerating islet-derived protein 3β (*Reg3β*) and regenerating islet-derived protein 3γ (*Reg3γ*) in the mouse colon in response to metronidazole administration ((15) and unpublished data). Metronidazole is a broad-spectrum antibiotic, which is highly active against gram-negative anaerobic microbes (16). It was first used by Shinn in 1962 to treat acute ulcerative gingivitis and more recently it has been extensively used in treating diseases such as IBD and *Clostridium difficile* infection (17). The colonic mucosal barrier plays an important role in protecting epithelium integrity and functionality. The secretion of mucus, which is predominated by secretory mucin MUC2, as well as other components such as antimicrobial peptides and immunoglobulins forms a complex biochemical matrix to maintain a dynamic and healthy barrier (13)(14). The C-type lectin Reg3β and Reg3γ are members of the REG gene family, which are antimicrobial peptides synthesized by Paneth cells in the small intestine and by crypt epithelium

in the colon (18), and are a key element of host defence supporting the mucosal barrier (19). *Reg3β* and *Reg3γ* have been reported to influence host-commensal and host-pathogen interactions in the GI tract, and regulate innate immune response (20, 21). It has been shown that metronidazole treatment significantly increased the expression of *Reg3γ* in the distal colon of mice, indicating increased microbial stimulation of the epithelium and weakened mucosal barrier (15). However, in subsequent unpublished studies we have observed reduced *Reg3γ* expression in response to metronidazole treatment. It was noted that in studies where *Reg3γ* dropped in response to metronidazole, there was a lack of *Escherichia coli,* whereas in experiments where *Reg3γ* increased, *E. coli* flourished in response to metronidazole treatment. Therefore, we hypothesized that the initial commensal microbiota, particularly the presence or absence of *E. coli*, contributed to the difference in host response to metronidazole treatment. In this study it is shown that the addition of a single commensal *E. coli* results in a distinct pattern of microbial shift and host response after metronidazole treatment. While this study focuses on a single commensal organism and a single antibiotic, it was designed as a proof of concept study to demonstrate that variations in membership of the pre-existing microbiota impact the subsequent changes in microbial composition as well as host response to antibiotic treatment.

MATERIALS AND METHODS

Mice. 6-8-week-old C57BL/6J female mice (Jackson Laboratory, Bar Harbor, ME) were housed in the animal facilities at the University of Alberta. Mice were kept in filter-topped cages, fed autoclaved food and water, and handled in biosafety cabinet under specific pathogen-free (SPF) conditions. Mice were randomly grouped into eight cages with 4 mice per cage by a blinded lab animal technician and balanced for average body weight. The cages were allocated to 4 treatments: control (CON), *E. coli* colonization (EC), metronidazole treatment (MET), and

metronidazole treatment after *E. coli* colonization (EC-MET). The protocol of the study is shown in Figure 1A1. Briefly, mice from the group EC and EC-MET were exposed to a commensal *E. coli* by oral gavage, while group CON and MET received PBS. 10 days post colonization, MET and EC-MET mice were given metronidazole (Sigma-Aldrich, Oakville, ON) at 750 mg/liter in drinking water for 4 days, while the CON and EC groups continued on sterilized water. Mice were euthanized after 4 days of metronidazole/water administration and tissues were harvested. The experiment was repeated 3 times with the sample size of 4, 8, and 8, respectively (n = 20 in total).

To further investigate whether effects of metronidazole on *E. coli* abundance and host response were transient or long-term, twenty mice were randomly grouped into eight cages with 2 or 3 mice per cage. The cages were allocated to 4 treatments as described above (n = 5). The procedure is shown in Figure 1A2 for the 14 day metronidazole treatment. Additionally, in order to study if the host response to metronidazole administration with the presence of *E. coli* is unique to the specific strain studied, two additional commensal *E. coli* were added to repeat the protocol as shown in Figure 1A1. Forty mice were randomly grouped into 16 cages with 2 or 3 mice per cage. The cages were allocated to 6 treatments (n = 5): control (CON), wild mice *E. coli* isolate colonization (WMEC), rat *E. coli* isolate colonization (REC), metronidazole treatment (MET), metronidazole treatment after wild mice *E. coli* isolate colonization (WMEC-MET) and after rat mice *E. coli* isolate colonization (REC-MET). The protocols employed were approved by the University of Alberta's Animal Care Committee and in direct accordance with the guideline of the Canadian Council on the Use of Laboratory Animals.

Bacterial strains. The commensal *E. coli* strains were isolated from a healthy NIH Swiss mouse (Harlan Laboratories, Inc., Indianapolis, IN), a wild mouse feces (glycerol stock), and rat feces

on MacConkey agar. The bacterial strains were cultivated in 5 mL of Luria-Bertani (LB) medium (Fisher Scientific, Nepean, ON) at 37℃ for 16 h. The culture medium containing approximately 2.0×10^8 colony forming units (CFU)/mL of *E. coli* was centrifuged at 5,000 x g for 10 min to harvest the bacterial cells. The pellets of *E. coli* cells were suspended in 1 x PBS and the mice were exposed to *E. coli* by oral gavage with 0.1 mL of suspension. Enumeration of *E. coli* was conducted by serial dilutions of fecal samples plated on MacConkey agar (BD, Sparks, MD) and total CFUs per gram fecal contents were then calculated.

Whole genome sequencing and annotation. To determine whether the *E. coli* isolated from a healthy mouse had any known virulence factors the genome was sequenced. Whole genome sequences of the isolated commensal *E. coli* strain were generated on the Illumina Miseq Platform. Illumina fragment libraries were generated using Nextera XT DNA Library Preparation Kit (Illumina, San Diego, CA) and quantified by Qubit 2.0 Fluorometer (Invitrogen, Carlsbad, CA). Libraries were normalized to 2 nM and denatured using 0.1 N NaOH and mixed with 5% PhiX genomic DNA as positive control. The sequencing flow cell cluster amplification was performed with 2 x 300 base paired-end reads on Illumina MiSeq instrument, using the V3 MiSeq sequencing-by-synthesis kits (Illumina, San Diego, CA). The draft genome was assembled with the SPAdes assembler (22) and the Rapid Annotations using Subsystems Technology (RAST) (23) was used for genome annotation. IslandViewer was used for predicting toxin-related virulence in the whole genome of the *E. coli* isolate (24).

Tissue collection. Four days or 14 days after metronidazole treatment, mice were euthanized by CO_2 asphyxiation followed by cervical dislocation. The terminal 5 mm piece of distal colon was collected for histological analysis and the remaining colon tissue was harvested for subsequent gene expression and cytokine analysis. Colonic contents were collected for microbial

composition analysis. All tissue samples were immediately placed in 10% neutral buffered formalin for histological studies or snap frozen in liquid nitrogen.

Microbial composition analysis. Total DNA was extracted from colonic contents using the QIA stool extraction kit (Qiagen Inc., Valencia, CA) with the addition of a bead-beating step as described in a previous study (25). Amplicon libraries were constructed from colonic content samples that amplified the V3-V4 region of the 16S rRNA gene according to the protocol from Illumina (16S Metagenomic Sequencing Library Preparation). Primers targeting the region were: (Forward: 5'-TCGTCGGCAGCGTCAGATGTGTATAAGAGACAGCCTACGGGNGGCWGCAG-3'; Reverse: 5'-GTCTCGTGGGCTCGGAGATGTGTATAAGAGACAGGACTACHVGGGTATCTAATCC-3'). A paired-end sequencing run was performed on the Illumina MiSeq Platform (Illumina Inc. San Diego, CA) using 2 x 300 cycles. The raw sequence data obtained was filtered through a quality control pipeline, and bases with quality scores lower than 33 were filtered using FASTX-Toolkit. Paired-end sequencing reads were merged using the PANDAseq algorithm. The QIIME 1.9.1 (Quantitative Insight into Microbial Ecology) toolkit and Usearch version 7.1 was applied for obtaining an operational taxonomic units (OUTs) table (26, 27) using the following procedures. First, merged sequences were dereplicated and filtered for chimaeras against the ChimeraSlayer reference database. Secondly, the high-quality reads were mapped against the database of usearch_global and the OTU table was obtained using the script of 'uc2otutab.py'. The classification of representative sequences for each OTU was carried out using the QIIME pipeline with the default algorithm of Ribosome Database Project (RDP) classifier (confidence threshold, 80%). The Greengenes (GG) v.13_8 reference database clustered at 97% identity was used for assigning taxonomy. The alpha diversity parameters for the microbial community,

including the Chao1 and Shannon index, were estimated by normalizing the number of sequences per sample to the lowest counts among all samples.

RNA isolation and cDNA synthesis. Colon tissue was excised, snap frozen in liquid nitrogen, and subsequently stored at -80℃ until RNA extraction. RNA was extracted using the GeneJET RNA Purification Kit (Thermo Scientific, Nepean, ON) following the manufacturer's instructions. RNA quality was verified by gel electrophoresis using 2x RNA GEL Loading Dye (Thermo Scientific, Nepean, ON). The concentration of RNA was determined by a NanoDrop ND-2000 spectrophotometer (NanoDrop Technologies, Wilmington, DE) and 1 μg RNA was used for reverse transcription (RT) using the Maxima First Strand cDNA Synthesis kit (Thermo Scientific, Nepean, ON).

Real-time PCR. Real-time PCR was performed using PerfeCTa SYBR Green Supermix (Quantabio, Gaithersburg, MD). Primers for host gene expression (*Reg3β*, *Reg3γ*, *MUC2*, and *IL-22*) are listed in Table 1. Real-time PCR was performed on an ABI StepOne™ real-time System (Applied Biosystems, Foster City, CA), and followed the cycles: 95℃ for 20 s and 40 cycles of 94℃ for 10 s, 60℃ for 30 s. Glyceraldehyde-3-phosphate dehydrogenase (*GAPDH*) was used as housekeeping gene for normalization. The fold change of gene expression compared to the control group was calculated using the $2^{-\Delta\Delta Ct}$ method.

Cytokine determination. For protein extraction, 50-100 mg snap frozen colon tissues were stored at -80℃ and subsequently homogenized in 150 μL RIPA buffer which contains 50 mM Tris-HCl (pH 8.0), 150 mM NaCl, 0.1% Triton X-100, 0.5% Sodium deoxycholate, 1 mM Sodium orthovanadate, 1 mM NaF, and Protease inhibitors cocktail (Sigma-Aldrich, Oakville, ON). The homogenates were centrifuged at 10, 000 x g for 20 min, and the supernatant was collected. Protein concentrations in the supernatant were determined using the Pierce BCA

protein assay kit (Thermo Scientific, Nepean, ON). The MSD Proinflammatory Panel 1 (mouse) kit (Meso Scale Discovery, Gaithersburg, MD) was used to quantify cytokines according to the manufacturer's recommendations with input protein concentration at 5 mg/mL. Cytokine concentrations were normalized to protein content.

Histology. The distal 5 mm of the colon were collected and immediately placed in 10% neutral buffered formalin at room temperature for 24 h, and then placed into 70% ethanol. Fixed tissue was embedded in paraffin, sectioned into 5 μm slices and subjected to hematoxylin and eosin (H&E) staining (15). Images were taken using an EVOS FL Auto Imaging System (Thermo Scientific, Nepean, ON). The well-oriented cross sections were assessed for pathology as previous described (15).

Statistical analysis and visualization. Data were analyzed in a completely randomized design and the fixed effects of the treatment in the model were *E. coli* presence, metronidazole treatment, and their interaction. Mouse was considered as the experimental unit. To compare the enumeration of *E. coli* at different time point, Kruskal-Wallis test was used to calculate *P* values and Dunn's test was used for multiple comparisons (SAS Inst. Inc., Cary, NC). Data of body weight, gene expression, cytokine and microbial abundance (regularized log (x + 1) transformed) were analyzed by PROC GLM with Bonferroni correction in SAS. Microbial diversity indices (Chao1 and Shannon) for each sample was calculated using the vegan package in R (R 3.3.2). Results are expressed as mean value with standard error of the mean (s.e.m.). Probability values less than 0.05 were considered as significant difference. Principle Component Analysis (PCA) derived from weighted UniFrac distance was performed to evaluate the overall differences between groups using the JMP software program (version 10.0.2, SAS Inst. Inc.). The permutational multivariate analysis of variance (adonis) was used to compare beta-diversity of

four groups based on Bray-Curtis dissimilarities with permutations number of 999 using R. Correlation of colonic *E. coli* bacterial load with tumor necrosis factor alpha (TNF-α) levels was analyzed by Spearman Rank Correlation using SAS. Graphpad Prism 6 software (Graphpad Software, Inc, La Jolla, CA) was used for data graphing.

Accession number(s). The whole genome sequences of the mice commensal *E. coli* isolate was deposited in the Sequence Read Archive (SRA) under accession number SUB2077929. Raw sequence reads of the 16S rRNA gene amplicon data are available through the SRA with accession number SUB2077113.

RESULTS

Metronidazole treatment stimulated an overgrowth of colonic commensal *E. coli*. A commensal *E. coli* was isolated from a fresh mouse fecal sample on MacConkey agar. The genome of the mouse *E. coli* isolate consisted of a single circular chromosome of 5,190,098 bp with an average GC content of 50.60%. The number of predicted unique genes encoded by the chromosome is 4,826. There were no identified hits of toxin virulence factors (VFs)-related genes in the genome of the *E. coli* isolate.

Wild-type C57BL/6 mice obtained from the Jackson laboratory were identified to be free of *E. coli* by selective culture of fecal samples on MacConkey agar. The commensal *E. coli* successfully colonized the mouse intestine with a single dose in the EC and EC-MET group, ranging from 2.22×10^5 to 2.25×10^6 CFU/g feces 2 days after exposure. The abundance varied from 1.07×10^5 to 6.21×10^6 CFU/g feces 10 days after *E. coli* treatment, indicating stability of *E. coli* colonization (Fig. 1B). Enumeration of *E. coli* in mice feces collected after 4 days metronidazole/water administration showed that *E. coli* were 6830-fold more abundant in the EC-MET group than the EC group (CFU/g feces) (Fig. 1B). Neither body weight loss nor death

253 was observed with colonization of *E. coli*. There were no differences in body weight between
254 metronidazole treated groups and vehicle control groups (Fig. 1C).
255 **Metronidazole treatment reduced enteric microbial biodiversity**. The intestinal microbiota
256 after 4 days metronidazole/water treatment were characterized by sequencing of 16S rRNA gene
257 tags (V3-V4 region) from colonic contents using Illumina MiSeq platform. The number of
258 sequencing reads obtained was 3,134,825, with an average of 101,123 ± 36,174 (mean ± SD)
259 quality-controlled and chimera-checked reads per sample. OTU clustering (97% cutoff) yielded a
260 total of 535 OTUs for the entire data set, which included 373 OTUs associated with CON dataset,
261 167 OTUs with the MET group, 262 OTUs with the EC-MET group, and 320 OTUs with the EC
262 group.
263 To evaluate phylogenetic richness and evenness of the intestinal microbiota, Chao1 diversity
264 index and Shannon index were calculated in each sample. The numbers of sequences per library
265 were normalized to 29,037 for the bacterial community according to the minimum reads number
266 among all libraries. *E. coli* x metronidazole interactions were observed in Chao1 ($P < 0.05$) and
267 Shannon indexes ($P < 0.01$) (Fig. 2A). The Chao1 index and Shannon values of the intestinal
268 microbiota in CON and EC were significantly higher than that in both metronidazole treated
269 groups, indicating a lower alpha diversity resulted from metronidazole treatment ($P < 0.05$) (Fig.
270 2A). When treated with metronidazole, the group with *E. coli* colonization showed a greater
271 reduction in alpha diversity than the MET group (Shannon index, $P < 0.05$; Fig. 2A).
272 **Overall structural changes of gut microbiota in response to metronidazole treatment**. To
273 assess the abundance profile of different phyla and genera, all sequences were assigned to
274 taxonomy using RDP Classifier. There were significant differences between groups at different
275 taxonomic levels. Bacteroidetes was the most predominant phyla in the CON and EC groups,

276 contributing the average of 77.8% and 72.6% of the microbial communities, respectively.
277 Firmicutes was the next most dominant phyla, representing an average of 21.5% and 26.2%,
278 respectively. In MET group, the most abundant phylum was Firmicutes (71.7%), while
279 Actinobacteria (23.2%) and Verrucomicrobia (4.6%) constituted the next most abundant phyla.
280 However, in EC-MET group, Proteobacteria was the dominant phylum with 81.8% of the
281 microbiota, and with much less Firmicutes (10.1%), Actinobacteria (6.2%), and Bacteroidetes
282 (1.8%) (Fig. 2B). Principal component analysis based on weighted UniFrac distance revealed a
283 distinct clustering of MET and EC-MET groups but no separation of CON and EC group based
284 on the first two principal component (PC) scores, which accounted for 88.30% and 9.82% of the
285 total variation, respectively (Fig. 3A). The permutational multivariate analysis of variance
286 (adonis) exhibited the separation of MET and EC-MET groups from the CON and EC group ($P <$
287 0.01).
288 Multivariate analysis performed on the OTUs suggested that colonization of *E. coli* isolate did
289 not result in major shifts in microbial composition compared to the microbial profile in CON
290 group. The most profound changes were enrichment of the genera of *Allobaculum* (0.65% vs.
291 0.04%, $P < 0.01$), *Akkermansia* (0.85% vs. 0.2%, $P < 0.01$), *Lactobacillus* (2.16% vs. 0.76%, $P <$
292 0.01), and *Ruminococcus* (0.66% vs. 0.29%, $P < 0.01$) in EC vs. CON (Fig. 2B). In addition, the
293 microbiota in the MET group underwent profound losses ($P < 0.05$) of the genera of
294 *Clostridiales_unclassified* and *Rikenellaceae_unclassified* and became dominated by
295 *Lactobacillus*, *Bifidobacterium*, *Enterococcaceae_unclassified*, *Turicibacter*, and *Akkermansia*
296 species in comparison to CON and EC group (Fig. 2B; Fig. 3B). However, with the presence of
297 *E. coli*, metronidazole treatment induced a distinct pattern of microbial composition. The EC-
298 MET group showed marked expansion of the *Enterobacteriaceae* proportions (represented by

only the inoculated *E. coli*) compared to the EC group (81.74% vs. 0.02%) and contractions of previously dominant populations, which were substantial for *Bacteroidales_S24-7_unclassified* and *Clostridiales_unclassified*, and modest for *Turicibacter* (Fig. 2B; Fig. 3B). The presence of *E. coli* and metronidazole administration interacted in producing significant effects on the abundance of certain bacterial families including *Bifidobacteriaceae*, *Lactobacillaceae*, *Enterococcaceae*, and *Enterobacteriaceae* (Fig. 3B). The distinct effect of metronidazole on colonic microbial composition confirms that the alterations in bacterial communities were highly dependent on the presence of *E. coli* before antibiotic administration.

Because analysis of microbial composition is based on relative abundance, and the increase in *E. coli* alone could reduce relative abundance of other taxa without reducing their actual number, the microbiota of EC-MET to MET groups were compared with the OTU representing *E. coli* removed. Even with *E. coli* removed from the analysis, community composition based on beta-diversity was still significantly different between EC-MET and MET groups (adonis analysis, $P < 0.05$; permutations number of 999). In addition, there were differences in the abundance of some genera between metronidazole treated groups including reduced abundance of Turicibacteraceae in the EC-MET group (17.9 ± 5.81%, mean ± s.e.m.) compared to the MET (0.69 ± 0.23%, mean ± s.e.m.) group.

Host response to metronidazole treatment is driven by corresponding initial bacterial composition. As mentioned above, our previous studies in mice showed inconsistent changes in mRNA expression of host antimicrobial protein Reg3γ in response to metronidazole treatment. Based on the hypothesis that the pre-existing gut microbiota may play a role in driving the difference in host response towards antibiotics administration, the mRNA expression of *Reg3β*, *Reg3γ*, *MUC2*, and *IL-22* were analyzed using real-time PCR. As shown in Figure 4A, EC-MET

mice exhibited a significant increase in mRNA expression of both *Reg3β* and *Reg3γ* compared to that in CON group ($P < 0.05$). Mice without *E. coli* colonization showed substantial variation (7.94 ± 4.43 fold change, mean ± s.e.m.) in *Reg3β* mRNA expression level in response to metronidazole treatment whereas the group with *E. coli* showed a consistent increase in *Reg3β* expression (13.07 ± 2.07 fold change, mean ± s.e.m.) with metronidazole treatment (Fig. 4A). In contrast, the increased mRNA expression of *Reg3γ* in response to metronidazole treatment was tightly associated with the enrichment of *E. coli* (Fig. 4B). It has been reported that metronidazole treatment induced a reduction in *MUC2* mRNA expression and a thinning of the mucus layer in the distal colon in mice (15). In the current study, colonization of *E. coli* tended to stimulate the mRNA expression of *MUC2* ($0.05 < P \leq 0.1$) (Fig. 4C). Although the MET group had slightly lower expression levels of *MUC2* mRNA, there was no significant difference between the MET and CON group in *MUC2* expression. There was no significant change in *IL-22* expression detected in the MET, EC, and EC-MET group compared to CON ($P > 0.05$, Fig. 4D).

To determine whether increased *Reg3β* and *Reg3γ* expression was associated with intestinal inflammation, colonic cytokines were measured by ELISA. The most profound change in colonic cytokine profile was the level of TNF-α, as shown in Figure 5A1. TNF-α was induced in EC-MET mice as compared to all other treatment groups ($P < 0.01$). There was an *E. coli* x metronidazole interaction for the expression level of TNF-α ($P < 0.05$), which indicated that the combination of *E. coli* and metronidazole was required to drive this response. Metronidazole treatment in the absence of *E. coli* did not increase TNF-α, however did increase the expression level of IL-1β ($P < 0.05$), IL-6 ($P < 0.01$), and IL-10 ($P < 0.01$) (Fig. 5B).

344 The correlation between enriched *E. coli* abundance in the EC-MET group and levels of TNF-α
345 was analyzed using Spearman's rank correlation. As shown in Figure 5A2, there was a trend for
346 TNF-α expression levels to be correlated with colonic *E. coli* counts ($r = 0.643$, $P = 0.096$).
347 Collectively, there was a clear pattern of increased pro-inflammatory cytokines in *E. coli*
348 colonized mice in response to metronidazole administration (TNF-α), though the histological
349 analysis of distal colon sections from all groups did not show significant evidence of
350 inflammation (Fig. 6). In contrast, with the absence of *E. coli*, the MET group did not exhibit
351 upregulation of TNF-α. The results suggest that the immune homeostatic imbalance of colonic
352 epithelium triggered by metronidazole treatment was driven by initial commensal microbial
353 composition profile.
354 In the long-term metronidazole treatment experiment, the stimulating effects of metronidazole on
355 colonic commensal *E. coli* growth was stable (Fig. 7A1). The abundance of *E. coli* after
356 metronidazole treatment for 14 days ranged from 1.50×10^8 to 2.08×10^{10} CFU/g feces, whereas
357 the abundance of *E. coli* in the group that received water for 14 days varied from 7.50×10^4 to
358 9.44×10^5 CFU/g feces (Fig. 7A1). With the overgrowth of *E. coli* during the long-term
359 metronidazole administration, the expression level of *Reg3β* and *Reg3γ* mRNA persisted ($P <$
360 0.05) (Fig. 7A2 & A3).
361 The commensal *E. coli* strains isolated from wild mouse and healthy rat stably colonized the
362 mouse intestine with an average abundance of 5.57×10^6 and 1.15×10^5 CFU/g feces,
363 respectively. Four-day metronidazole treatment significantly increased the abundance of *E. coli*
364 to an average of 3.35×10^9 and 1.24×10^9 CFU/g feces, in WMEC-MET and REC-MET
365 respectively (Fig. 7B1 & C1). In the wild mouse *E. coli* isolate colonized mice, metronidazole
366 administration also increased ($P < 0.05$) the expression level of *Reg3β* and *Reg3γ* mRNA, which

were 2.8- and 7.7-fold change respectively compared to the levels in the CON group (Fig 7B2 & B3). However, in the rat *E. coli* isolate colonized mice, metronidazole did not significantly affect the expression of these two genes in conjunction with *E. coli* proliferation (Fig 7C2 & C3).

DISCUSSION

The results of this study show that the pre-existing composition of commensal microbes plays an important role in how the host responds to antibiotic treatment. In particular, the presence or absence of a commensal *E. coli* impacts mucosal immunity of the colon and alters the shifts in microbial composition induced by metronidazole treatment. Our current study showed that metronidazole administration dramatically reduced the biodiversity of the gut microbiota, as indicated by Chao1 and Shannon index. Changes in the microbiome, largely reflected an increase in *E. coli,* which induced expression of genes coding antimicrobial peptides and inflammation.

It is well recognized that broad-spectrum antibiotics significantly reduce the richness and evenness of the intestinal microbiota (28, 29). In the current study, we have observed lower biodiversity in gut microbiota after a four-day metronidazole treatment. Within the metronidazole treated mice, the presence of *E. coli* accelerated the reduction in diversity of the gut microbiota, as indicated by Shannon index. The observation suggested that the gut microbial composition before metronidazole treatment could be predictive of the degree of reduction in diversity, at least for this specific antibiotic administration.

Previously published studies have shown that metronidazole treatment induced a significant disturbance in the microbial composition of the colon, targeting depletion of obligate anaerobic *Bacteroidales* communities (15, 16, 31). Consistent with previous findings, the comparison of MET group and CON group exhibited a dramatic decrease in relative abundance of the genera *Bacteroidales_S24-7.* Studies in humans and animal models have demonstrated that broad-

spectrum antibiotics targeting specific pathogenic organisms can influence the commensal microbial community to a much greater degree than previously assumed. A recent study, which used metronidazole and vancomycin to treat wild-type C57Bl/6 mice from Jackson Laboratory, showed that the genus of *Enterococcus*, *unclassified_Proteobacteria*, novel members of *Lactobacillus* and *Clostridium* greatly expanded with metronidazole treatment, while *Lactobacillus aviaries*, *Enterococcus faecalis*, *Klebsiella oxytoca*, and *Akkermansia muciniphilia* expanded with vancomycin. Moreover, the authors observed that the expanding populations were highly dependent on the initially colonized communities (31). Another study reported that a single dose of clindamycin treatment for one day in mice resulted in generally similar expansions and contractions of gut microbiota, but occasional differences between individuals were observed. The authors concluded that these differences between individuals were likely due to the subtle differences in the initial commensal microbiota (32). Concordant with the previous studies, we observed a great expansion of *Enterococcus*, *Lactobacillus* and *Clostridium* compared to the initial point in the MET group. In addition, the presence of commensal *E. coli* resulted in a very different expansion, showing the remarkable effects of a subtle difference in initial microbiota. It has been widely recognized that the composition of human gut microbiota varies among individuals as a result of different selection pressure from the host, microbial ecosystem, and environment. Therefore, it is essential to be aware of the initial difference when evaluating the outcome from antibiotic treatments.

In the current study, there was a distinct host response to metronidazole treatment with respect to innate immunity as well as mucosal homeostasis due to the addition of a single commensal organism to the initial microbiota. Evidence has correlated changes of host innate mucosal immunity with commensal microorganisms in previous studies. Acute colonisation with

commensal Schaedler's *E. coli* in immune competent germ-free BALB/c mice resulted in 1.6-3.5-fold induction of *Reg3β* and *Reg3γ* and no induction of IFN-γ (33). In the current study, the addition of *E. coli* alone did not result in increased expression of *Reg3β* and *Reg3γ*. This likely reflects the much greater degree to which *E. coli* will colonize in a germ-free as compared to conventional animal (34). Interestingly, in another study where germ free C57/Bl6 mice were monocolonized with a non-host adapted commensal *E. coli* JM83 strain for three weeks, *Reg3γ* expression was not increased (35), indicating *E. coli* must be somewhat host-adapted and have the ability to penetrate to the mucosal surface to elicit this response. It has been reported that *Lactobacillus reuteri* exhibited different host-adapted lineages in mice, indicating the evolutional host-driven diversification (36). In addition, a study using a germ-free mouse model colonized with single commensal bacteria clearly showed that *Reg3γ* is not driven by an enriched total number of bacteria but triggered by increased microbial-epithelial contact at the mucosal surface (18). The increased expression of *Reg3β* and *Reg3γ* genes have been associated with an inflammatory response and bacterial reconstitution, which was accompanied with strengthened communication between gut commensal bacteria and mucosal surface (37). In the current study, the elicited expression of *Reg3β* and *Reg3γ* genes in the EC-MET (both 4 days and 14 days) and WMEC-MET group is likely due to increased contact between commensal bacteria and the mucosal surface, which is stimulated by the imbalanced microbiota to fortify epithelial barrier function. The lack of increase observed in *Reg3β* and *Reg3γ* genes in REC-MET group may reveal that host-adaptation is a prerequisite for the stimulation of gut epithelium by gut commensal bacteria.

Evidence suggests that IL-22 is a key element for directly inducing the expression of Reg3γ in the colon (38, 39), however increased IL-22 was not observed in the current study. It has been

436 shown that *Bifidobacterium breve* NCC2950 induced Reg3γ in the absence of IL-22, implying
437 that the induction of the Reg3 family involves multiple pathways (35). Therefore, the induced
438 expression of *Reg3β* and *Reg3γ* in the current study is likely through a non-IL-22 mediated
439 mechanism.
440 Metronidazole treatment of C57BL/6 mice has previously been shown to reduce the mRNA
441 expression of *MUC2*, which resulted in a thinner mucus layer (15). However, it has been
442 reported that metronidazole administration in rats increased bacteria penetrating the crypts and a
443 thickening of the mucus layer in the proximal colon (40). In the current study, *E. coli*
444 colonization significantly increased the expression of *MUC2* while metronidazole treatment
445 didn't impact the expression of the gene. This difference may be explained by the nature of the
446 shifts in the microbiome seen in the previous rat study as compared to the current study;
447 supporting the concept that response to antibiotic treatment will vary depending on the pre-
448 existing microbiota.
449 An array of cytokines was analyzed in the colon of mice in response to antibiotic treatment as an
450 indicator of intestinal inflammation. The results showed a trend for a correlation between *E. coli*
451 enrichment and expression of TNF-α. Studies in different models, especially *in vitro* cell culture,
452 have reported the stimulation of inflammatory cytokines by commensal bacteria. It has been
453 reported that a commensal *E. coli* strain stimulated Caco-2 cells to produce TNF-α and IL-1β,
454 but did not induce secretion of IFN-γ, IL-4, or IL-12 in Caco-2 cells (41). The increase of TNF-α
455 expression by commensal *E. coli* has been shown in HT-29 cell line model as well (42). TNF-α
456 is a proinflammatory cytokine for which expression is enhanced by a variety of stimuli such as
457 bacterial endotoxin (LPS) (43). The changes in this proinflammatory related cytokine in the
458 current study suggest that with the acute and strong expansion of commensal *E. coli* in response

to metronidazole treatment, the microbial changes triggered an imbalance in immune homeostasis. The immune homeostatic imbalance is likely due to the increase in contact between commensal bacteria and intestinal epithelium resulting from *E. coli* expansion, and in turn, the imbalance in immune homeostasis may further exaggerate the alterations of the gut microbiota. While the relationship between *E. coli* and metronidazole is of direct interest, this study provides proof of concept in how care must be taken using antibiotics as a study tool since the differences in results from one experiment to the next can be attributed to the pre-existing microbiota. Furthermore, the study demonstrated that initial gut microbial composition is a key factor driving host response to antibiotics administration, creating a compelling argument to consider personalized medication based on individual variation in gut microbiota.

ACKNOWLEDGMENTS

We thank Kunimasa Suzuki from Molecular Biology Core at Alberta Diabetes Institute for his technical assistance with cytokine analysis. T. Ju was supported by a Graduate Student Scholarship from the Alberta Innovates-Technology Futures, Alberta, Canada. B.P.W. is supported by the Canada Research Chair Program.

FUNDING INFORMATION

This research was supported by a Natural Sciences and Engineering Research Council Discovery grant held by B.P.W..

REFERENCES

1. **Sartor RB**. 2004. Therapeutic manipulation of the enteric microflora in inflammatory bowel diseases: Antibiotics, probiotics, and prebiotics. Gastroenterology.
2. **Jernberg C**, **Löfmark S**, **Edlund C**, **Jansson JK**. 2007. Long-term ecological impacts of

antibiotic administration on the human intestinal microbiota. ISME J **1**:56–66.

3. **Jernberg C**, **Löfmark S**, **Edlund C**, **Jansson JK**. 2010. Long-term impacts of antibiotic exposure on the human intestinal microbiota. Microbiology.

4. **Willing BP**, **Russell SL**, **Finlay BB**. 2011. Shifting the balance: antibiotic effects on host-microbiota mutualism. Nat Rev Microbiol **9**:233–243.

5. **Langdon A**, **Crook N**, **Dantas G**. 2016. The effects of antibiotics on the microbiome throughout development and alternative approaches for therapeutic modulation. Genome Med **8**:39.

6. **Colombel JF**, **Lemann M**, **Cassagnou M**, **Bouhnik Y**, **Duclos B**, **Dupas JL**, **Notteghem B**, **Mary JY**. 1999. A controlled trial comparing ciprofloxacin with mesalazine for the treatment of active Crohn's disease. Groupe d'Etudes Therapeutiques des Affections Inflammatoires Digestives (GETAID). Am J Gastroenterol **94**:674–678.

7. **Arnold GL**, **Beaves MR**, **Pryjdun VO**, **Mook WJ**. 2002. Preliminary study of ciprofloxacin in active Crohn's disease. Inflamm Bowel Dis **8**:10–5.

8. **Guslandi M**. 2005. Antibiotics for inflammatory bowel disease: do they work? Eur J Gastroenterol Hepatol **17**:145–147.

9. **Hu Y**, **Yang X**, **Qin J**, **Lu N**, **Cheng G**, **Wu N**, **Pan Y**, **Li J**, **Zhu L**, **Wang X**, **Meng Z**, **Zhao F**, **Liu D**, **Ma J**, **Qin N**, **Xiang C**, **Xiao Y**, **Li L**, **Yang H**, **Wang J**, **Yang R**, **Gao GF**, **Wang J**, **Zhu B**. 2013. Metagenome-wide analysis of antibiotic resistance genes in a large cohort of human gut microbiota. Nat Commun **4**:2151.

10. **Dethlefsen L**, **Huse S**, **Sogin ML**, **Relman DA**. 2008. The pervasive effects of an antibiotic on the human gut microbiota, as revealed by deep 16s rRNA sequencing. PLoS Biol **6**:2383–2400.

11. **Dethlefsen L**, **Relman DA**. 2011. Incomplete recovery and individualized responses of the human distal gut microbiota to repeated antibiotic perturbation. Proc Natl Acad Sci U S A 4554–61.

12. **Raymond F**, **Ouameur A a**, **Déraspe M**, **Iqbal N**, **Gingras H**, **Dridi B**, **Leprohon P**, **Plante P-L**, **Giroux R**, **Bérubé È**, **Frenette J**, **Boudreau DK**, **Simard J-L**, **Chabot I**, **Domingo M-C**, **Trottier S**, **Boissinot M**, **Huletsky A**, **Roy PH**, **Ouellette M**, **Bergeron MG**, **Corbeil J**. 2015. The initial state of the human gut microbiome determines its reshaping by antibiotics. ISME J 1–14.

13. **Van der Sluis M**, **De Koning BAE**, **De Bruijn ACJM**, **Velcich A**, **Meijerink JPP**, **Van Goudoever JB**, **Büller HA**, **Dekker J**, **Van Seuningen I**, **Renes IB**, **Einerhand AWC**. 2006. Muc2-Deficient Mice Spontaneously Develop Colitis, Indicating That MUC2 Is Critical for Colonic Protection. Gastroenterology **131**:117–129.

14. **Zarepour M**, **Bhullar K**, **Montero M**, **Ma C**, **Huang T**, **Velcich A**, **Xia L**, **Vallance BA**. 2013. The mucin muc2 limits pathogen burdens and epithelial barrier dysfunction during salmonella enterica serovar typhimurium colitis. Infect Immun **81**:3672–3683.

15. **Wlodarska M**, **Willing B**, **Keeney KM**, **Menendez A**, **Bergstrom KS**, **Gill N**, **Russell SL**, **Vallance BA**, **Finlay BB**. 2011. Antibiotic treatment alters the colonic mucus layer and predisposes the host to exacerbated Citrobacter rodentium-induced colitis. Infect Immun **79**:1536–1545.

16. **Löfmark S**, **Edlund C**, **Nord CE**. 2010. Metronidazole is still the drug of choice for treatment of anaerobic infections. Clin Infect Dis **50**:16–23.

17. **Eykyn SJ**, **Phillips I**. 1976. Metronidazole and anaerobic sepsis. BrMedJ **2**:1418–1421.

18. **Vaishnava S**, **Yamamoto M**, **Severson KM**, **Ruhn KA**, **Yu X**, **Koren O**, **Ley R**,

Wakeland EK, **Hooper L V**. 2011. The Antibacterial Lectin RegIIIgamma Promotes the Spatial Segregation of Microbiota and Host in the Intestine. Science (80-) **334**:255–258.

19. **Hiemstra PS**. 2001. Epithelial antimicrobial peptides and proteins: Their role in host defence and inflammation. Paediatr Respir Rev **2**:306–310.

20. **Cash HL**, **Whitham C V**, **Behrendt CL**, **Hooper L V**. 2006. Symbiotic bacteria direct expression of an intestinal bactericidal lectin. Science **313**:1126–30.

21. **Brandl K**, **Plitas G**, **Schnabl B**, **DeMatteo RP**, **Pamer EG**. 2007. MyD88-mediated signals induce the bactericidal lectin RegIIIγ and protect mice against intestinal Listeria monocytogenes infection. J Exp Med **204**:1891–1900.

22. **Bankevich A**, **Nurk S**, **Antipov D**, **Gurevich A a.**, **Dvorkin M**, **Kulikov AS**, **Lesin VM**, **Nikolenko SI**, **Pham S**, **Prjibelski AD**, **Pyshkin A V.**, **Sirotkin A V.**, **Vyahhi N**, **Tesler G**, **Alekseyev M a.**, **Pevzner P a.** 2012. SPAdes: A New Genome Assembly Algorithm and Its Applications to Single-Cell Sequencing. J Comput Biol **19**:455–477.

23. **Aziz RK**, **Bartels D**, **Best AA**, **DeJongh M**, **Disz T**, **Edwards RA**, **Formsma K**, **Gerdes S**, **Glass EM**, **Kubal M**, **Meyer F**, **Olsen GJ**, **Olson R**, **Osterman AL**, **Overbeek RA**, **McNeil LK**, **Paarmann D**, **Paczian T**, **Parrello B**, **Pusch GD**, **Reich C**, **Stevens R**, **Vassieva O**, **Vonstein V**, **Wilke A**, **Zagnitko O**. 2008. The RAST Server: rapid annotations using subsystems technology. BMC Genomics **9**:75.

24. **Dhillon BK**, **Laird MR**, **Shay JA**, **Winsor GL**, **Lo R**, **Nizam F**, **Pereira SK**, **Waglechner N**, **McArthur AG**, **Langille MGI**, **Brinkman FSL**. 2015. IslandViewer 3: More flexible, interactive genomic island discovery, visualization and analysis. Nucleic Acids Res **43**:W104–W108.

25. **Willing BP**, **Vacharaksa A**, **Croxen M**, **Thanachayanont T**, **Finlay BB**. 2011. Altering

host resistance to infections through microbial transplantation. PLoS One **6**. e26988.

26. **Caporaso JG**, **Kuczynski J**, **Stombaugh J**, **Bittinger K**, **Bushman FD**, **Costello EK**, **Fierer N**, **Peña AG**, **Goodrich JK**, **Gordon JI**, **Huttley GA**, **Kelley ST**, **Knights D**, **Koenig JE**, **Ley RE**, **Lozupone CA**, **McDonald D**, **Muegge BD**, **Pirrung M**, **Reeder J**, **Sevinsky JR**, **Turnbaugh PJ**, **Walters WA**, **Widmann J**, **Yatsunenko T**, **Zaneveld J**, **Knight R**. 2010. QIIME allows analysis of high-throughput community sequencing data. Nat Methods **7**:335–6.

27. **Edgar RC**. 2010. Search and clustering orders of magnitude faster than BLAST. Bioinformatics **26**:2460–2461.

28. **Perez-Cobas AE**, **Gosalbes MJ**, **Friedrichs A**, **Knecht H**, **Artacho A**, **Eismann K**, **Otto W**, **Rojo D**, **Bargiela R**, **von Bergen M**, **Neulinger SC**, **Daumer C**, **Heinsen FA**, **Latorre A**, **Barbas C**, **Seifert J**, **Santos VM Dos**, **Ott SJ**, **Ferrer M**, **Moya A**, **Pérez-Cobas AE**, **Bergen M Von**, **Däumer C**, **Martins V**, **Dos Santos VM**. 2012. Gut microbiota disturbance during antibiotic therapy: a multi-omic approach. Gut **62**:1–11.

29. **Francino MP**. 2016. Antibiotics and the human gut microbiome: Dysbioses and accumulation of resistances. Front Microbiol.

30. **Gerritsen J**, **Smidt H**, **Rijkers GT**, **De Vos WM**. 2011. Intestinal microbiota in human health and disease: The impact of probiotics. Genes Nutr.

31. **Lewis BB**, **Buffie CG**, **Carter RA**, **Leiner I**, **Toussaint NC**, **Miller LC**, **Gobourne A**, **Ling L**, **Pamer EG**. 2015. Loss of Microbiota-Mediated Colonization Resistance to Clostridium difficile Infection With Oral Vancomycin Compared With Metronidazole. J Infect Dis **212**:1656–65.

32. **Buffie CG**, **Jarchum I**, **Equinda M**, **Lipuma L**, **Gobourne A**, **Viale A**, **Ubeda C**,

Xavier J, **Pamer EG**. 2012. Profound alterations of intestinal microbiota following a single dose of clindamycin results in sustained susceptibility to Clostridium difficile-induced colitis. Infect Immun **80**:62–73.

33. **Keilbaugh S a**, **Shin ME**, **Banchereau RF**, **McVay LD**, **Boyko N**, **Artis D**, **Cebra JJ**, **Wu GD**. 2005. Activation of RegIIIbeta/gamma and interferon gamma expression in the intestinal tract of SCID mice: an innate response to bacterial colonisation of the gut. Gut **54**:623–9.

34. **Willing BP**, **Van Kessel AG**. 2007. Enterocyte proliferation and apoptosis in the caudal small intestine is influenced by the composition of colonizing commensal bacteria in the neonatal gnotobiotic pig. J Anim Sci **85**:3256–3266.

35. **Natividad JMM**, **Hayes CL**, **Motta JP**, **Jury J**, **Galipeau HJ**, **Philip V**, **Garcia-Rodenas CL**, **Kiyama H**, **Bercik P**, **Verd?? EF**. 2013. Differential induction of antimicrobial REGIII by the intestinal microbiota and Bifidobacterium breve NCC2950. Appl Environ Microbiol **79**:7745–7754.

36. **Oh PL**, **Benson AK**, **Peterson DA**, **Patil PB**, **Moriyama EN**, **Roos S**, **Walter J**, **Lantbruksuniversitet S**. 2010. Diversification of the gut symbiont lactobacillus reuteri as a result of host-driven evolution. ISME J **4**:377–387.

37. **Loonen LMP**, **Stolte EH**, **Jaklofsky MTJ**, **Meijerink M**, **Dekker J**, **van Baarlen P**, **Wells JM**. 2014. REG3γ-deficient mice have altered mucus distribution and increased mucosal inflammatory responses to the microbiota and enteric pathogens in the ileum. Mucosal Immunol **7**:939–47.

38. **Zheng Y**, **Valdez PA**, **Danilenko DM**, **Hu Y**, **Sa SM**, **Gong Q**, **Abbas AR**, **Modrusan Z**, **Ghilardi N**, **de Sauvage FJ**, **Ouyang W**. 2008. Interleukin-22 mediates early host

defense against attaching and effacing bacterial pathogens. Nat Med **14**:282–9.

39. **Sanos SL**, **Vonarbourg C**, **Mortha A**, **Diefenbach A**. 2011. Control of epithelial cell function by interleukin-22-producing RORgammat+ innate lymphoid cells. Immunology **132**:453–465.

40. **Pélissier MA**, **Vasquez N**, **Balamurugan R**, **Pereira E**, **Dossou-Yovo F**, **Suau A**, **Pochart P**, **Magne F**. 2010. Metronidazole effects on microbiota and mucus layer thickness in the rat gut. FEMS Microbiol Ecol **73**:601–610.

41. **Haller D**, **Bode C**, **Hammes WP**, **Pfeifer AM**, **Schiffrin EJ**, **Blum S**. 2000. Non-pathogenic bacteria elicit a differential cytokine response by intestinal epithelial cell/leucocyte co-cultures. Gut **47**:79–87.

42. **Bahrami B**, **Macfarlane S**, **Macfarlane GT**. 2011. Induction of cytokine formation by human intestinal bacteria in gut epithelial cell lines. J Appl Microbiol **110**:353–363.

43. **De Plaen IG**, **Tan XD**, **Chang H**, **Wang L**, **Remick DG**, **Hsueh W**. 2000. Lipopolysaccharide activates nuclear factor kappaB in rat intestine: role of endogenous platelet-activating factor and tumour necrosis factor. Br J Pharmacol **129**:307–14.

44. **Goodrich ME**, **McGee DW**. 1999. Effect of intestinal epithelial cell cytokines on mucosal B-cell IgA secretion: Enhancing effect of epithelial-derived IL-6 but not TGF-?? on IgA+ B cells. Immunol Lett **67**:11–14.

45. **Vinderola G**, **Matar C**, **Perdigon G**. 2005. Role of intestinal epithelial cells in immune effects mediated by gram-positive probiotic bacteria: involvement of toll-like receptors. Clin Diagn Lab Immunol **12**:1075–84.

46. **Kuhn KA**, **Manieri NA**, **Liu TC**, **Stappenbeck TS**. 2014. IL-6 stimulates intestinal epithelial proliferation and repair after injury. PLoS One **9**.

47. **Curtis MM**, **Hu Z**, **Klimko C**, **Narayanan S**, **Deberardinis R**, **Sperandio V**. 2014. The gut commensal bacteroides thetaiotaomicron exacerbates enteric infection through modification of the metabolic landscape. Cell Host Microbe **16**:759–769.

48. **Hoebler C**, **Gaudier E**, **De Coppet P**, **Rival M**, **Cherbut C**. 2006. MUC genes are differently expressed during onset and maintenance of inflammation in dextran sodium sulfate-treated mice. Dig Dis Sci **51**:381–389.

49. **Satoh-Takayama N**, **Serafini N**, **Verrier T**, **Rekiki A**, **Renauld JC**, **Frankel G**, **DiSanto J**. 2014. The chemokine receptor CXCR6 controls the functional topography of interleukin-22 producing intestinal innate lymphoid cells. Immunity **41**:776–788.

Figure legends

Figure. 1. Experimental protocol. *E. coli*: Re-suspend bacteria in PBS with a concentration of 2.0 x 10^8 CFU/mL was given to mice (0.1 mL/each mouse). Metronidazole: 750 mg/L in drinking water. Body weight was recorded weekly. Mice were sacrificed on **A1**) Day 4 or **A2**) Day 14. **B**) Enumeration of *E. coli* in mouse feces before metronidazole treatment and 4 days after metronidazole/water administration. Dots represent individual mice and lines depict the mean values. **C**) Body weight change during the *E. coli* treatment and 4 days metronidazole/water treatment. For all treatment groups, n = 8. Data are shown as mean ± s.e.m. ^{a,b} Means that do not share a common letter are significantly different. $\alpha = 0.05$.

Figure. 2. **A**) Alpha diversity analysis of bacterial communities in colon contents of mice. All the colonic content were harvested after 4 days metronidazole/water administration. Data are shown as mean ± s.e.m. ^{a,b,c} Means that do not share a common letter are significantly different. $\alpha = 0.05$.

643 **B**) Bar chart indicating microbial community profiles between groups, summarized down to the
644 genus level. Microbial composition of the four groups before experimental treatment are labeled
645 as CON_PRE, MET_PRE, EC_MET_PRE, EC_PRE, respectively.
646
647 Figure. 3. **A**) Principle component analysis (PCA) plots of the bacterial communities based on
648 the weighted UniFrac distance matrix. Each plot point represents an individual mouse. **B**) Box-
649 plots show selective bacterial abundance in different treated groups at family level. Colonic
650 contents were collected after 4 days metronidazole/water treatment. For all treatment groups, n =
651 8. Data are shown as mean ± s.e.m. [a,b,c] Means that do not share a common letter are significantly
652 different. $\alpha = 0.05$.
653
654 Figure. 4. Quantitative RT-PCR results of **A**) *Reg3β*, **B**) *Reg3γ*, **C**) *Muc2*, and **D**) *IL-22*
655 expression in the colon of untreated, *E. coli* and metronidazole-treated mice. Colonic tissue
656 samples were harvested after 4 days metronidazole/water administration. For all treatment group,
657 n = 8. Data are shown as mean ± s.e.m. [a,b,c] Means that do not share a common letter are
658 significantly different. $\alpha = 0.05$.
659
660 Figure. 5. Cytokine analysis results of **A1**) TNF-α, **B1**) IL-1β, **B2**) IL-6, **B3**) IL-10 production in
661 the colon. Colonic tissue samples were collected after 4 days metronidazole/water treatment. For
662 all treatment groups, n = 8. Data are shown as mean ± s.e.m. [a,b,c] Means that do not share a
663 common letter are significantly different. $\alpha = 0.05$. **A2**) Correlation of colonic *E. coli* bacterial
664 load with TNF-α expression levels in EC-MET group. Spearman's correlation coefficient (r
665 values) and significance *P* values are shown.

Figure. 6. Distal colon sections from CON, MET, EC, and EC-MET mice 4 days after metronidazole/water treatment were stained with Haematoxylin and Eosin. There is no significant inflammation evidence in all treatments, including inflammation and damage of lumen, surface epithelium, mucosa, and submucosa, as well as the number of goblet cells. Original magnification and bars: Left: x 40, 1000 μm; right: x 400, 100 μm.

Figure. 7. Enumeration of *E. coli* in mouse feces and colonic gene expression of mice colonized with **A**) commensal *E. coli* isolates, **B**) wild mouse *E. coli* isolate, and **C**) rat *E. coli* isolate. For enumeration of *E. coli* in mouse feces, samples were taken before metronidazole treatment and after **A1**) 14 days or **B1, C1**) 4 days of metronidazole/water treatment. Dots represent individual mice and lines depict the mean values. *Reg3β* and *Reg3γ* expression in the colon of untreated, *E. coli* and metronidazole-treated mice was detected by quantitative RT-PCR. Colonic tissue samples were harvested after **A2**, **A3**) 14 days or **B2**, **B3**, **C2**, **C3)** 4 days metronidazole/water administration. For all treatment groups, n = 5. Data are shown as mean ± s.e.m. ^{a,b} Means that do not share a common letter are significantly different. $\alpha = 0.05$.

Table 1. Primers and thermal cycling profiles for real-time PCR analysis

Targeted genes	Oligonucleotides sequences (5'-3')	Annealing Tm (℃)	References
Reg3β	Forward: GGCTTCATTCTTGTCCTCCA	60	(47)
	Reverse: TCCACCTCCATTGGGTTCT		
Reg3γ	Forward: AAGCTTCCTTCCTGTCCTCC	60	(47)
	Reverse: TCCACCTCTGTTGGGTTCAT		

MUC2	Forward: GCTGACGAGTGGTTGGTGAATG	60	(48)
	Reverse: GATGAGGTGGCAGACAGGAGAC		
IL-22	Forward: TTGAGGTGTCCAACTTCCAGCA	60	(49)
	Reverse: AGCCGGACGTCTGTGTTGTTA		
GAPDH	Forward: ATTGTCAGCAATGCATCCTG	60	(15)
	Reverse: ATGGACTGTGGTCATGAGCC		

686

687 Figure 1

688

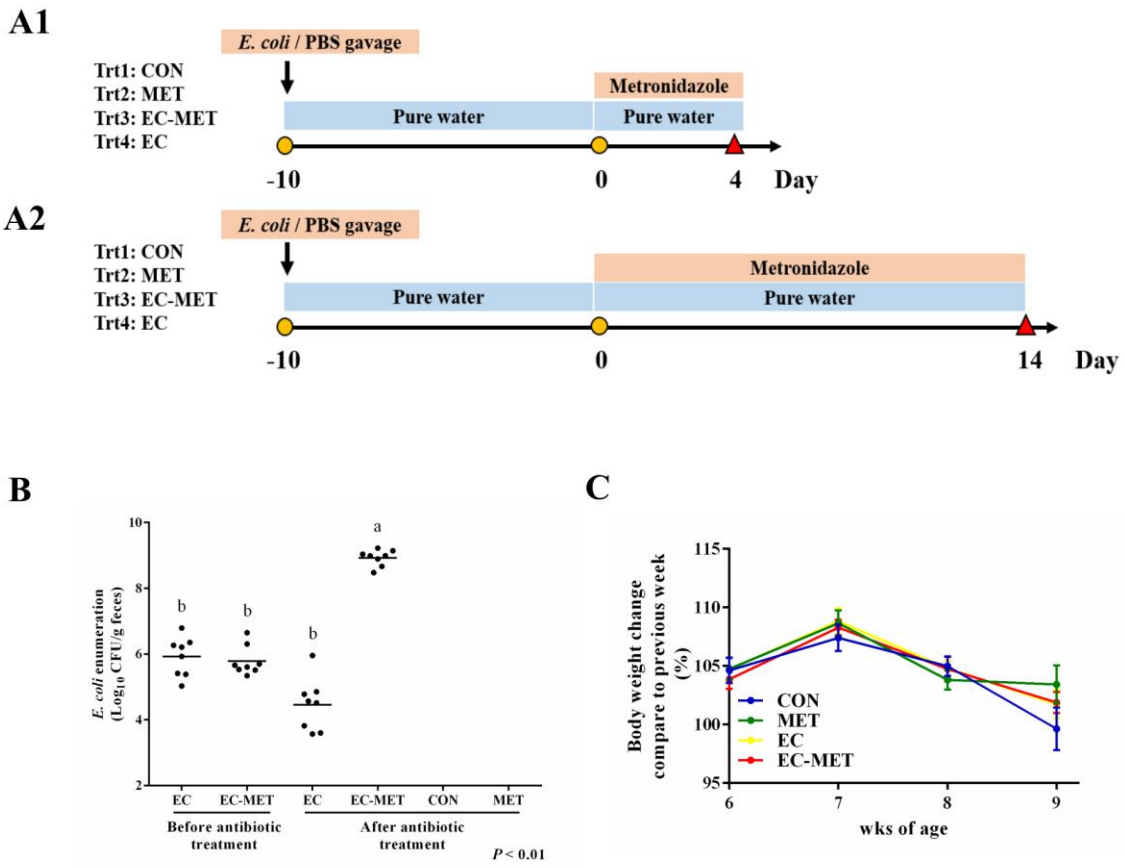

689 Figure 2

690

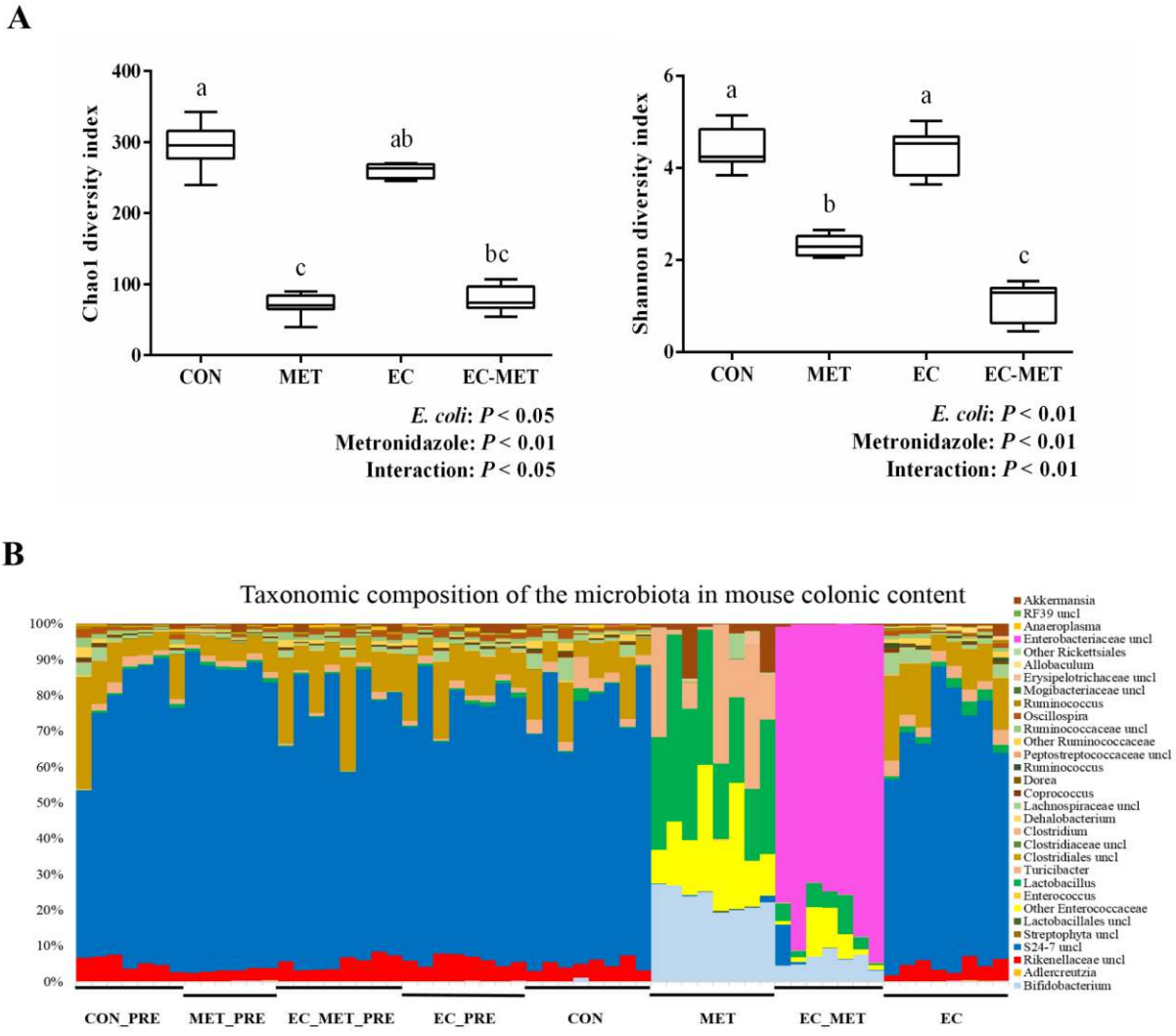

Figure 3

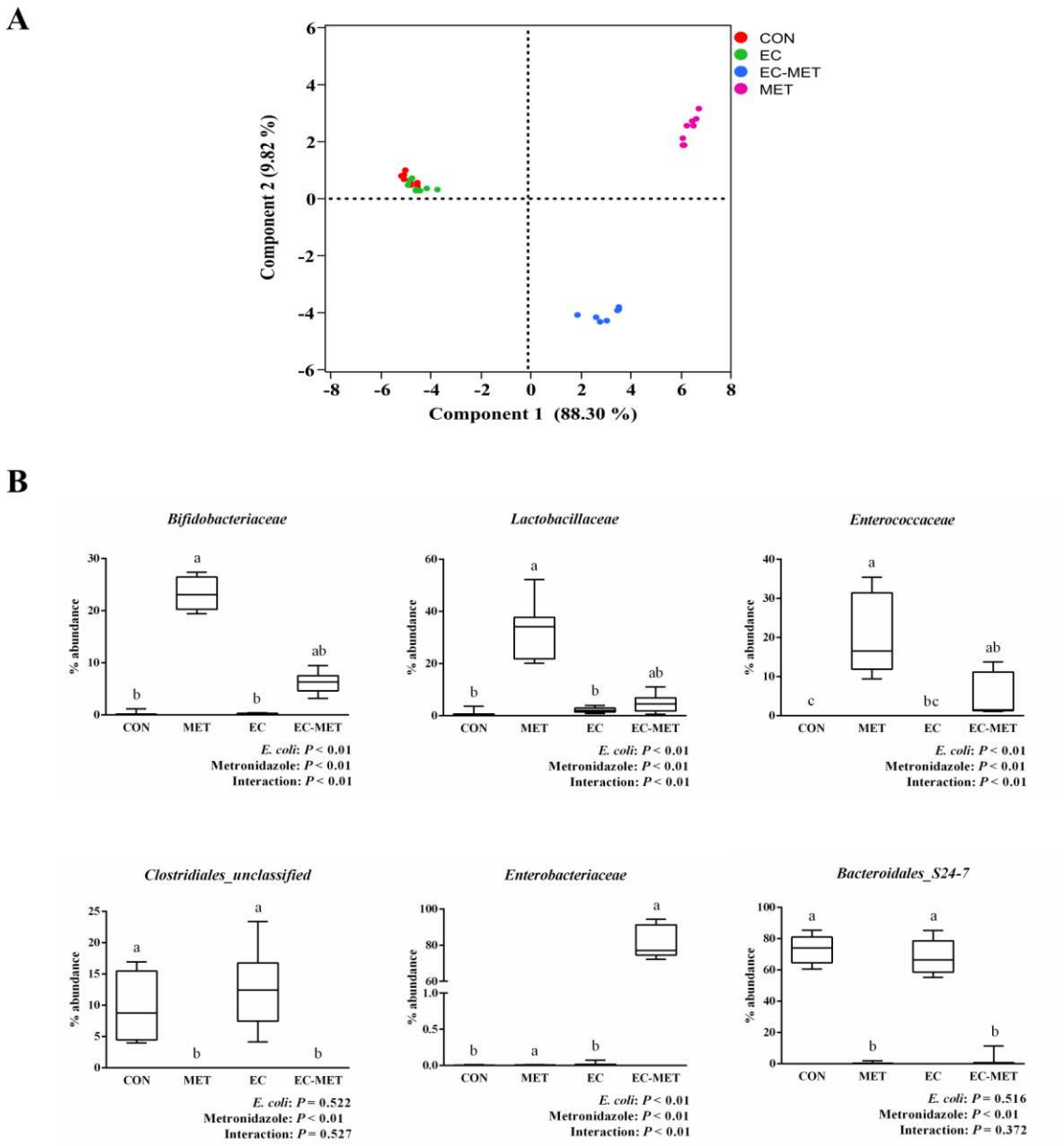
A
CON
EC
EC-MET
MET
Component 2 (9.82 %)
Component 1 (88.30 %)
B
Bifidobacteriaceae
Lactobacillaceae
Enterococcaceae
Clostridiales_unclassified
Enterobacteriaceae
Bacteroidales_S24-7
% abundance
CON
MET
EC
EC-MET
E. coli: P < 0.01
Metronidazole: P < 0.01
Interaction: P < 0.01
E. coli: P = 0.522
Metronidazole: P < 0.01
Interaction: P = 0.527
E. coli: P = 0.516
Metronidazole: P < 0.01
Interaction: P = 0.372

Figure 4

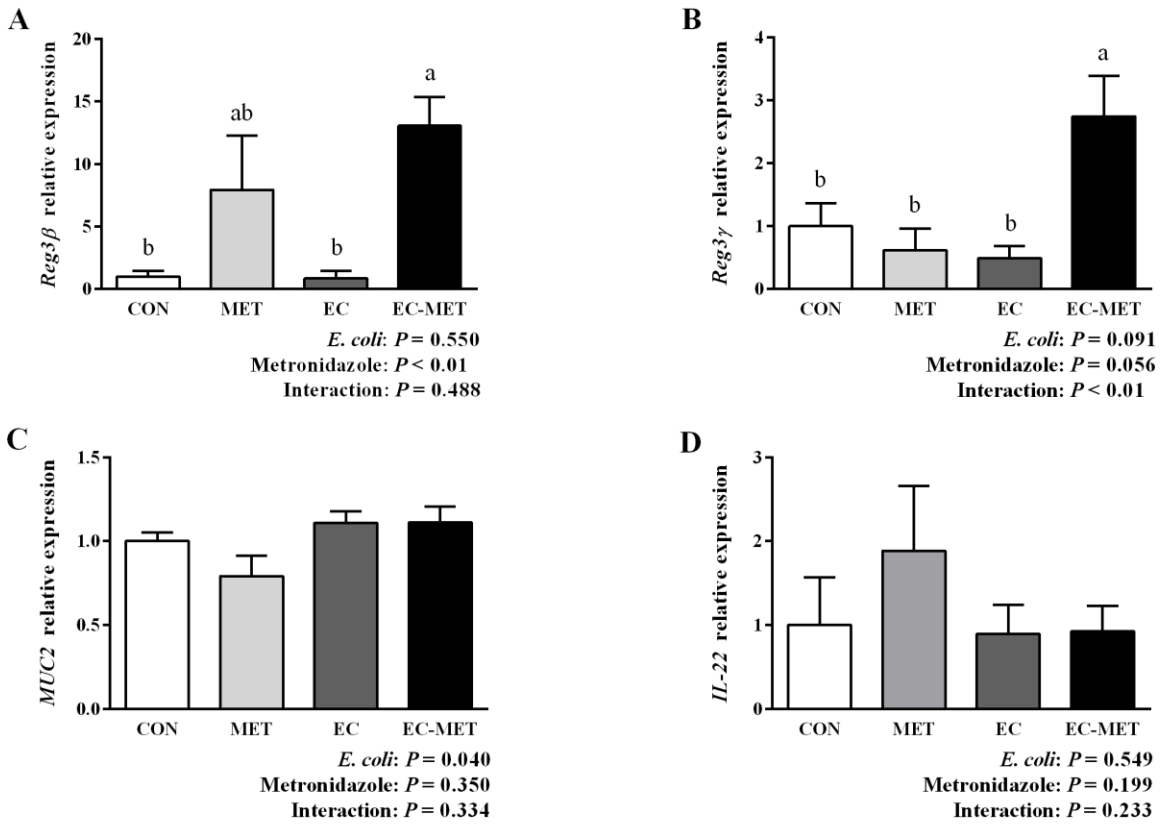
A
Reg3β relative expression
20
15
10
5
0
b
ab
b
a
CON
MET
EC
EC-MET
E. coli: P = 0.550
Metronidazole: P < 0.01
Interaction: P = 0.488
B
Reg3γ relative expression
4
3
2
1
0
b
b
b
a
CON
MET
EC
EC-MET
E. coli: P = 0.091
Metronidazole: P = 0.056
Interaction: P < 0.01
C
MUC2 relative expression
1.5
1.0
0.5
0.0
CON
MET
EC
EC-MET
E. coli: P = 0.040
Metronidazole: P = 0.350
Interaction: P = 0.334
D
IL-22 relative expression
3
2
1
0
CON
MET
EC
EC-MET
E. coli: P = 0.549
Metronidazole: P = 0.199
Interaction: P = 0.233

Figure 5

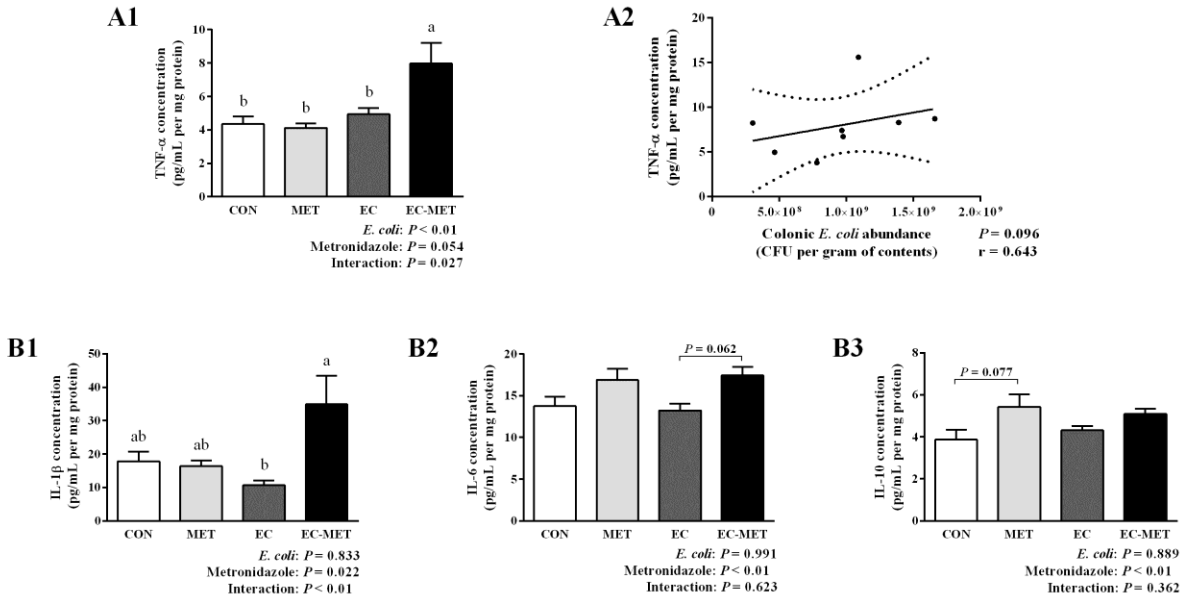
A1
TNF-α concentration (pg/mL per mg protein)
CON
MET
EC
EC-MET
E. coli: P < 0.01
Metronidazole: P = 0.054
Interaction: P = 0.027
A2
TNF-α concentration (pg/mL per mg protein)
Colonic E. coli abundance (CFU per gram of contents)
P = 0.096
r = 0.643
B1
IL-1β concentration (pg/mL per mg protein)
E. coli: P = 0.833
Metronidazole: P = 0.022
Interaction: P < 0.01
B2
IL-6 concentration (pg/mL per mg protein)
P = 0.062
E. coli: P = 0.991
Metronidazole: P < 0.01
Interaction: P = 0.623
B3
IL-10 concentration (pg/mL per mg protein)
P = 0.077
E. coli: P = 0.889
Metronidazole: P < 0.01
Interaction: P = 0.362

Figure 6

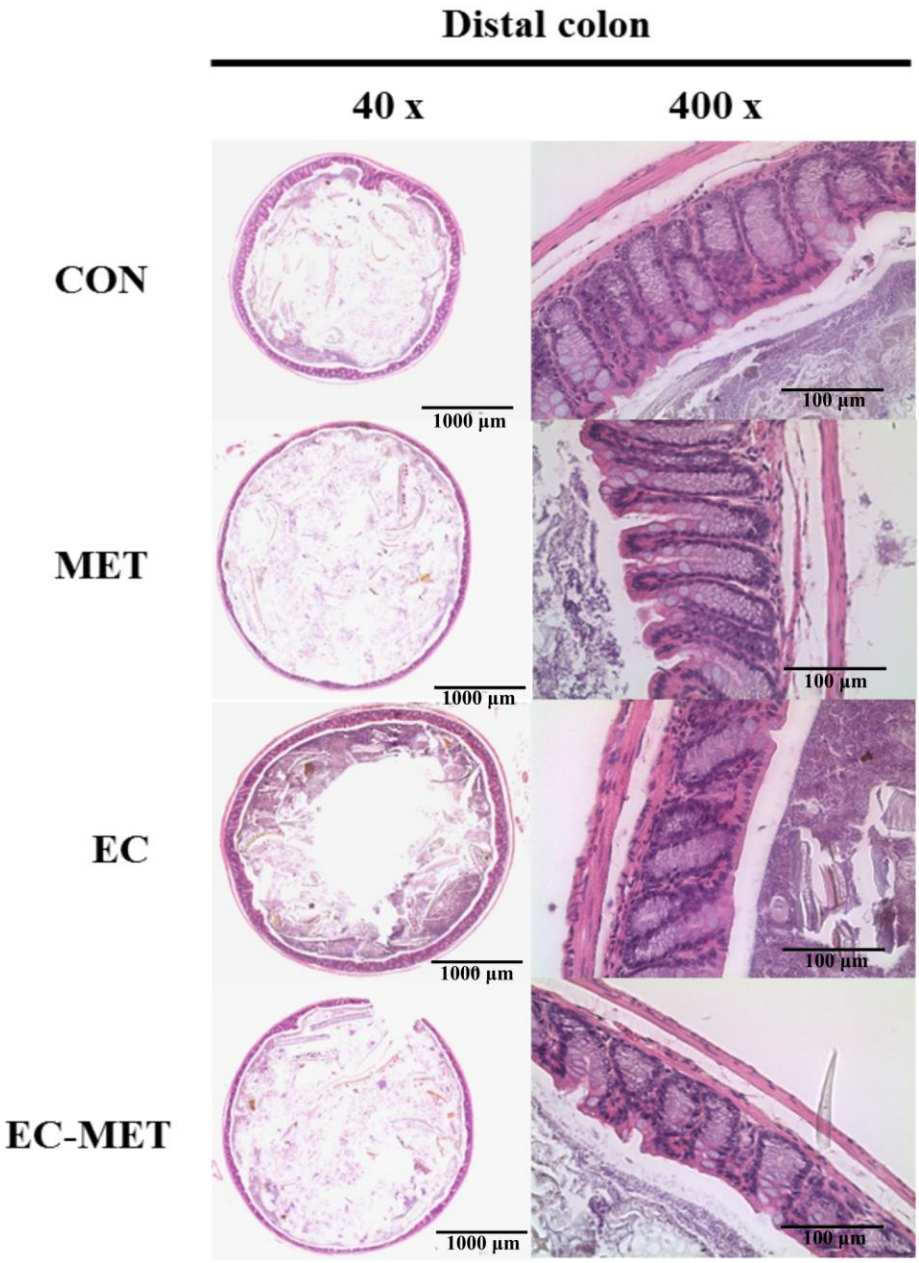

Figure 7

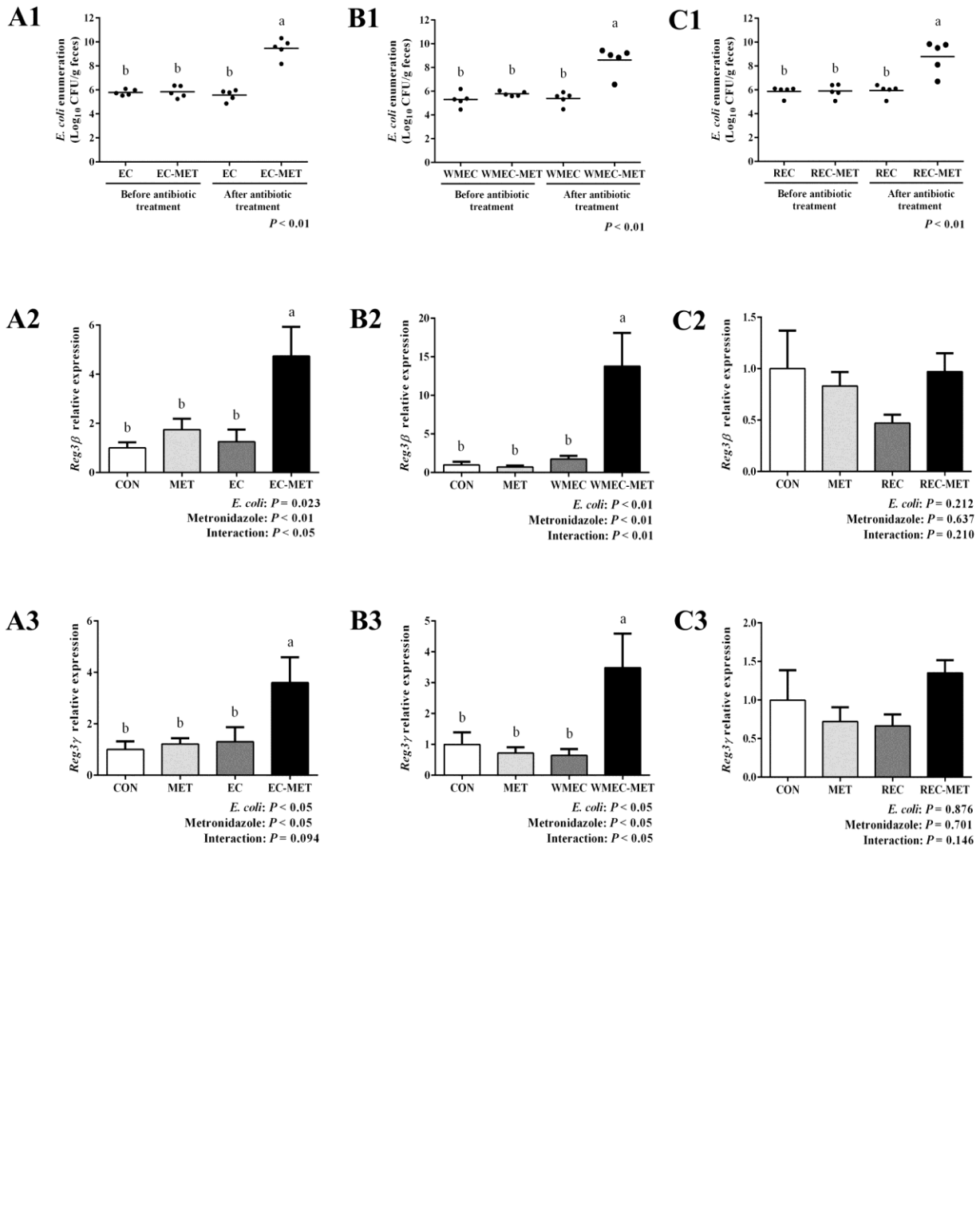
A1
E. coli enumeration (Log10 CFU/g feces)
EC EC-MET EC EC-MET
Before antibiotic treatment
After antibiotic treatment
P < 0.01
B1
E. coli enumeration (Log10 CFU/g feces)
WMEC WMEC-MET WMEC WMEC-MET
Before antibiotic treatment
After antibiotic treatment
P < 0.01
C1
E. coli enumeration (Log10 CFU/g feces)
REC REC-MET REC REC-MET
Before antibiotic treatment
After antibiotic treatment
P < 0.01
A2
Reg3β relative expression
CON MET EC EC-MET
E. coli: P = 0.023
Metronidazole: P < 0.01
Interaction: P < 0.05
B2
Reg3β relative expression
CON MET WMEC WMEC-MET
E. coli: P < 0.01
Metronidazole: P < 0.01
Interaction: P < 0.01
C2
Reg3β relative expression
CON MET REC REC-MET
E. coli: P = 0.212
Metronidazole: P = 0.637
Interaction: P = 0.210
A3
Reg3γ relative expression
CON MET EC EC-MET
E. coli: P < 0.05
Metronidazole: P < 0.05
Interaction: P = 0.094
B3
Reg3γ relative expression
CON MET WMEC WMEC-MET
E. coli: P < 0.05
Metronidazole: P < 0.05
Interaction: P < 0.05
C3
Reg3γ relative expression
CON MET REC REC-MET
E. coli: P = 0.876
Metronidazole: P = 0.701
Interaction: P = 0.146